On Couple Stress Effects on Unsteady Nanofluid Flow over Stretching Surfaces with Vanishing Nanoparticle Flux at the Wall

F. Awad[1, 2†], N. A. H. Haroun[2, 3], P. Sibanda[3] and M. Khumalo[1]

[1] *Department of pure & applied mathematics, university of Johannesburg, P.O. Box 524, Auckland Park 2006, Johannesburg, South Africa*
[2]*Department of Mathematics, Omdurman. I. University, Omdurman, Khartoum, Sudan*
[3]*School of Mathematics, Statistics and Computer Science, University of KwaZulu-Natal, Bag X01, Scottsville, Pietermaritzburg,3209, South Africa*

†*Corresponding Author Email: awad.fga@gmail.com*

ABSTRACT

In this paper the problem of unsteady nanofluid flow over a stretching sheet subject to couple stress effects is presented. Most previous studies have assumed that the nanoparticle volume fraction at the boundary surface may be actively controlled. However, a realistic boundary condition for the nanoparticle volume fraction model is that the nanoparticle flux at the boundary be set to zero. This paper differs from previous studies in that we assume there is no active control of the nanoparticle volume fraction at boundary. The spectral relaxation method has been used to solve the governing equations, moreover the results were further confirmed by using the quasi-linearization method. The qualitative and quantitative effects of the dimensionless parameters in the problem such as the couple stress parameter, the Prandtl number, the Brownian motion parameter, the thermophoresis parameter, the Lewis number on the fluid behavior are determined.

Keywords: Nanofluid; Couple stress; Stretching surface; Vanishing nanoparticle flux; Spectral relaxation method.

NOMENCLATURE

b& *c* are	positive constants with dimensions time^{-1}	α_m	effective thermal diffusivity
		η	similarity variable
D_B	Brownian diffusion coefficient	θ	Dimensionless temperature
D_T	thermophoresis diffusion coefficient	$v = \frac{\mu}{\rho}$	kinematic viscosity of the fluid
f	dimensionless velocity	$v' = \frac{\varsigma}{\rho}$	couple stress viscosity
g	acceleration due to gravity		
i	time index during navigation	ς	couple stress viscosity coefficient
L	scale	ρ	fluid density v
Le	Lewis number	μ	fluid viscosity
N	number of grid points	$(\rho c)_f$	effective heat capacity of the fluid
N_B	Brownian motion parameter	$(\rho c)_p$	effective heat capacity of the nanoparticle material
N_T	thermophoresis parameter		
p	fluid pressure	τ	parameter defined by $(\rho c)_f/(\rho c)_p$
Pr	Prandtl number	ϕ	Dimensionless nanoparticles volume
S	unsteadiness parameter		
t	time	$\widehat{\phi}$	nanoparticle volume concentration
T	fluid temperature	$\widehat{\phi}_\infty$	ambient nanoparticle volume fraction
T_w	temperature at the stretching surface		
T_∞	ambient fluid temperature		
T_{ref}	reference temperature	ω	Gauss-Lobatto points
u & v	velocity components (along xand y)	U	stretching velocity
Q_x	couple stress parameter	V = V(u, v)	fluid velocity
		x & y	Cartesian coordinates

1. INTRODUCTION

In the past few years, convective heat and mass transfer in nanofluids has become a topic of major interest. The thermal conductivity of a fluid plays an important role in the heat transfer between the fluid medium and a solid surface. Conventional heat transfer fluids including oil, water and ethylene glycol, etc., are poor heat transfer fluids due to low thermal conductivities. Nanofluids are engineered by suspending metallic nanoparticles with sizes below $100nm$ in traditional heat transfer fluids. Heat transfer enhancement using nanofluids in convective boundary-layer flow over a vertical plate, stretching sheet and moving surfaces has been studied by numerous authors, and are discussed in the review papers Buongiorno (2006), Oztop and Abu-Nada (2008), Daungthongsuk and Wongwises (2007, Nield and Kuznetsov (2009), Kuznetsov and Nield (2010a), Kuznetsov and Nield (2010b), Ahmad and Pop (2010), Khan and Pop (2010), Bachok, Ishak, and Pop (2010)andRashidi *et al.* (2014).

The couple stress fluid model is one of numerous viscoelastic models that have been proposed to describe the characteristics and Behavior of non-Newtonian fluids. The constitutive equations of these fluids are often very complex involving a large number of parameters. The couple stress fluid model is the simplest generalization of the classical theory of fluids which allows for polar effects such as couple stresses and body couples in the fluid medium. The theory of couple stress fluids was introduced in Stokes (1966) to explain the rheological behaviour of various complex non-Newtonian fluids with body stresses and body couples which cannot be treated by the classical theory of continuum mechanics. Due to the rotational interaction of particles, the force-stress tensor is not symmetric and the flow behaviour of such fluids is not similar to Newtonian fluids. Couple stress fluids have applications in engineering and chemical industries. The peristaltic transport of a couple stress fluid in an asymmetric channel with an induced magnetic field has been considered by Nadeem and Akram (2011). An analysis of the effects of couple stresses on the blood flow through a thin artery with a mild stenosis was carried out by Sinha and Singh (1984). Malashetty, Pop, Kollur, and Sidram (2012) investigated double diffusive convection in a couple stress fluid saturated porous layer with Soret effects. Hayat *et al.* (2013) observed that the velocity and the boundary layer thickness decrease with the couple stress fluid parameter in his study of melting heat transfer in the boundary layer flow of a couple stress fluid. Khan, Mahmood, and Ara (2013) found the approximate solution of the couple stress fluid between expanding and contracting walls. An analysis has been provided for three-dimensional magnetohydrodynamic flow of couple stress fluid with Newtonian heating by Ramzan, Farooq, Alsaedi, and Hayat (2013). Murthy and Nagaraju (2009) considered the flow of a couple stress fluid generated by a circular cylinder subjected to longitudinal and torsional oscillations, and the time dependence of the run up flow of a couple stress fluid between rigid parallel plates is examined by Devakar and Iyengar (2010) in which the flow was induced by a constant pressure gradient which is suddenly withdrawn and the parallel plates set to move instantaneously with different velocities in the direction of the applied pressure gradient. In this work we study the unsteady nanofluid flow over a stretching sheet in the presence of couple stress effects. To the best of our knowledge, most published work in the field of nanofluid, employed boundary conditions on the nanoparticle volume fraction analogous to those on the temperature thereby assuming that the nanoparticle volume fraction could be actively controlled at the boundary. A recent series of papers by Kuznetsov and Nield (2014), Nield and Kuznetsov (2014a), Nield and Kuznetsov (2014b), Nield and Kuznetsov (2014c) have suggested that a more realistic boundary condition is that the nanoparticle volume fraction flux at the boundary be set to zero. These boundary conditions have not been used on previous studies on couple stress fluids.

2. MATHEMATICAL FORMULATION

Consider the problem of two-dimensional flow of unsteady incompressible nanofluid over a stretching sheet subject to couple stress effect see Fig. (1).
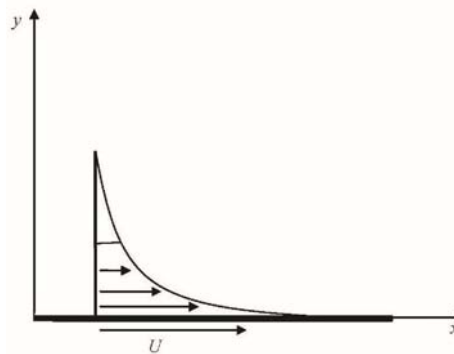

Fig. 1. Schematic diagram for the problem.

The continuous sheet isplaced at $y = 0$ and moves parallel to the $x - axis$ with velocity,

$$U = \frac{bx}{1 - ct} \tag{1}$$

where b and c are constants and t represents time. The boundary layer temperature and nanoparticle volume concentration are$T$ and $\hat{\phi}$ respectively. The ambient fluid temperature and nanoparticle volume fraction are $T_\infty$and $\hat{\phi}_\infty$respectively. At the surface, both the nanofluid and the sheet arekept at a constant temperature T_w where $T_w > T_\infty$is for aheated stretching surface and $T_w < T_\infty$corresponds to acooled surface.The boundary layer equations

governing the flow of an incompressible couple stress fluid are (see Hayat *et al.* (2013))

$$div\ V = 0,\qquad(2)$$

$$\rho\frac{DV}{Dt} = -\nabla p - \mu(\nabla \times \nabla \times V)$$

$$-\varsigma(\nabla \times \nabla \times \nabla \times \nabla \times V)\qquad(3)$$

The continuity, momentum, energy and nanoparticles fraction equations for the nanofluid can be expressed as,

$$\frac{\partial u}{\partial x} + \frac{\partial v}{\partial y} = 0\qquad(4)$$

$$\frac{\partial u}{\partial t} + u\frac{\partial u}{\partial x} + v\frac{\partial u}{\partial x} = v\frac{\partial^2 u}{\partial y^2} - v'\frac{\partial^4 u}{\partial y^4},\qquad(5)$$

$$\frac{\partial T}{\partial t} + u\frac{\partial T}{\partial x} + v\frac{\partial T}{\partial y} = \alpha_m\frac{\partial^2 T}{\partial y^2} + \tau\left[D_B\frac{\partial\widehat\phi}{y}\frac{\partial T}{\partial y} + \frac{D_T}{T_\infty}\left(\frac{\partial T}{\partial y}\right)^2\right],\qquad(6)$$

$$\frac{\partial\widehat\phi}{\partial t} + u\frac{\partial\widehat\phi}{\partial x} + v\frac{\partial\widehat\phi}{\partial y} = D_B\frac{\partial^2\widehat\phi}{\partial y^2} + \frac{D_T}{T_\infty}\frac{\partial^2 T}{\partial y^2},$$

equations (4)-(7) are subject to the boundary conditions

$$(7)$$

$$v = 0,\ u = U,\ T = T_s,\ D_B\frac{\partial\widehat\phi}{\partial y} + \frac{D_T}{T_\infty}\frac{\partial T}{\partial y} = 0\ \ on\ y = 0\qquad(8)$$

$$u \to 0,\ T \to T_\infty, \widehat\phi \to \widehat\phi_\infty,\ as\ y \to \infty\qquad(9)$$

For two-dimensional flow, it is convenient to introduce the stream function $\psi(x,\ y,\ t)$ and the following similarity transformations $\psi(x, y, t) = \sqrt{\frac{bv}{1-ct}}xf(\eta),$

$$\eta = \sqrt{\frac{b}{v(1-ct)}}\ y,$$

$$T(x,y,t) = T_\infty + T_{ref}\left[\frac{bx^2}{2v}\right](1-ct)^{-\frac{3}{2}}\theta(\eta),$$

$$\widehat\phi(x,y,t) = \widehat\phi_\infty + C_{ref}\left[\frac{bx^2}{2v}\right](1-ct)^{-\frac{3}{2}}\phi(\eta),$$

Equations (5)-(7) can now be presented in the form

$$f''' - Qf^{(5)} + ff'' - f'^2 - S\left(f' + \frac{1}{2}\eta f''\right) = 0,\qquad(10)$$

$$\theta'' + Pr\left[f\theta' - 2f'\theta - \frac{S}{2}(3\theta + \eta\theta')\right] + N_b\phi'\theta' + N_t\theta'^2 = 0,\qquad(11)$$

$$\phi'' + Le\left[f\phi' - 2f' - \frac{S}{2}(3\phi + \eta\phi)\right] + \frac{N_t}{N_b}\theta'' = 0,\qquad(12)$$

with boundary conditions

$$f = 0,\ f' = \theta = 1,\ N_b\phi' + N_t\ \theta' = 0,\qquad(13)$$

$$f' \to 0,\ \theta \to 0,\ \phi \to 0\ as\ \eta \to \infty,\qquad(14)$$

where the couple stress parameter Q, the dimensionless measure of unsteadiness S, the Prandtl number Pr, the Brownian motion parameter

N_b, the thermophoresis parameter N_t and the Lewis number Le are defined as

$$Q_x = \frac{v'U}{v^2 x},\ S = \frac{c}{b},\ N_t = \frac{\tau D_T(T_w - T_\infty)}{T_\infty\alpha_m},$$

$$N_b = \frac{\tau D_B\widehat\phi_{ref}\left[\frac{bx^2}{2v}\right]}{\alpha_m}(1-ct)^{-\frac{3}{2}},$$

$$Pr = \frac{v}{\alpha_m},\ Le = \frac{v}{D_B},$$

3- NUMERICAL SOLUTION

In this section, we apply the spectral relaxation method (SRM) to solve the nonlinear ODEs (10) - (12) along with boundary conditions (13)-(14). For the implementation of the spectral collocation method, it is convenient to reduce the order of equation (10) from five to four. To this end, we set $f' = g$, so that equation (10) becomes

$$-Qg'''' + g'' + \left(f + \frac{1}{2}\eta\right)g' - Sg = g^2,$$

$$g(0) = 1,\ g(\infty) = 0,\qquad(15)$$

$$f' = g,\ f(0) = 0,\qquad(16)$$

The spectral relaxation method algorithm (see Motsa, Dlamini, and Khumalo (2012), Motsa and Makukula (2013), Motsa, Dlamini, and Khumalo (2013)) first decouples the system of equations (10) - (12). From the decoupled equations an iteration scheme is developed by evaluating linear terms in the current iteration level which is denoted by the subscript $r + 1$ and nonlinear terms in the previous iteration level denoted by the subscript r. Applying the SRM to (11) - (12) and (15) - (16) gives the following linear ordinary differential equations;

$$-Qg_{r+1}'''' + g_{r+1}'' + \left(f_r + \frac{1}{2}\eta\right)g_{r+1}' - Sg_{r+1} = g_r^2,\qquad(17)$$

$$f_{r+1}' = g_{r+1},\ f_{r+1}(0) = 0,\qquad(18)$$

$$\theta_{r+1}'' + Pr\left(f_{r+1} - \frac{1}{2}S\eta + N_b\phi_r'\right)\theta_{r+1}' - Pr\left(2g_{r+1} + \frac{3}{2}S\right)\theta_{r+1} = -N_t\theta_r'^2,\qquad(19)$$

$$\phi_{r+1}'' + Le\left(f_{r+1} - \frac{1}{2}S\eta\right)\phi_{r+1}' - Le\left(2g_{r+1} + \frac{3}{2}S\right)\phi_{r+1} = -\frac{N_t}{N_b}\theta_r'',\qquad(20)$$

$$g_{r+1}(0) = 1,\ \theta_{r+1}(0) = 1,\ N_b\phi_{r+1}'(0) + N_t\theta_{r+1}'(0) = 0,\qquad(21)$$

$$g_{r+1}(\infty) = 0,\ \theta_{r+1}(\infty) = 0,\ \phi_{r+1}(\infty) = 0.\qquad(22)$$

Starting from given initial approximations $f_0,\ g_0,\ \theta_0\ and\ \phi_0$, the iteration schemes (17) - 20) can be solved iteratively using a spectral collocation method. In applying the spectral collocation method, we find the unknown function at the collocation points by requiring that equations (17) - (20) be satisfied exactly at these points. A convenient set of collocation points are the Gauss-Lobatto points defined by

$$\omega_j = \cos\frac{\pi j}{N},\quad j = 0, 1, ..., N\qquad(23)$$

For convenience, in numerical computations, the semi-infinite domain is approximated by the truncated domain $[0, L]$ and using thelinear transformation $\eta = L(\omega + 1)/2$, we convert $[0, L]$ intothe interval $[-1,1]$ in which the spectral method can be used,where $L = \eta_\infty$ is a finite number selected to be largeenough to represent the behavior of the flow properties when η is very large. The derivative are defined as

$$\frac{df}{d\eta} = \sum_{k=0}^{N} D_{jk} f(\omega_k) = Df, \; j = 0, 1, \dots, N \quad (24)$$

where $N + 1$ is the number of collocation points,

$D = 2D/L \; and \; F = [f(\omega_0),$ $f(\omega_1), \dots, f(\omega_N)]^T$ is the vector of unknown functions at the collocation points. Applying the Chebyshevspectral collocation method to the system (17) - (20) we obtain the following matrix equations

$A_{1,r} g_{r+1} = R_{1,r}, \; g_{r+1}(\omega_N) = 1, g_{r+1}(\omega_0) = 0$
$Df_{r+1} = g_{r+1}, \; f_{r+1}(\omega_N) = 0,$
$A_{2,r} \theta_{r+1} = R_{2,r}, \; \theta_{r+1}(\omega_N) = 1,$
$\qquad\qquad \theta_{r+1}(\omega_0) = 0,$
$A_{3,r} \phi_{r+1} = R_{3,r}, N_b \phi_{r+1}(\omega_N) + N_t \phi_{r+1}(\omega_N)$
$\phi_{r+1}(\omega_0) = 0,$

where

$$A_{1,r} = -QD^4 + D^2 + diag\left[f_r - \tfrac{1}{2} S\eta\right] D -$$
$$SI, R_{1,r} = g_r^2 \quad (25)$$

$$A_{2,r} = D^2 + Pr \; diag\left[f_{r+1} - \tfrac{1}{2} S\eta + N_b \phi_r'\right] D -$$
$$\left[2f_{r+1} + \tfrac{3}{2} S\right] I, \; R_{2,r} = -N_t \theta_r'^2 \quad (26)$$

$$A_{3,r} = D^2 + Le \; diag\left[f_{r+1} - \tfrac{1}{2} S\eta\right] D -$$
$$\left[2f_{r+1} + \tfrac{3}{2} S\right] I, \; R_{3,r} = -\tfrac{N_t}{N_b} \theta_r'' \quad (27)$$

Here I is an $(N + 1) \times (N + 1)$ diagonal matrix and $diag$ [] denotes a diagonal matrix. Starting from stable initial approximations $f_0, \; g_0,$ $\theta_0 \; and \; \phi_0$ whichsatisfy the boundary conditions of governing equations:

$$f_0 = \left(\tfrac{\eta^2}{6} - 1\right) e^{-\eta} \quad (28)$$

$$g_0 = \left(1 + \tfrac{\eta}{3} - \tfrac{\eta^2}{6}\right) e^{-\eta} \quad (29)$$

$$\theta_0 = e^{-\eta}, \; \phi_0 = -\tfrac{N_t}{N_b} e^{-\eta} \quad (30)$$

4- RESULTS AND DISCUSSION

To obtain clear insights into the physics of the problem of unsteady nanofluid flow over a stretching sheet with couple stresses, the set of ordinary differential equations (10) – (12) were solved using the spectral relaxation method. We determined through numerical experimentation that $\eta_\infty = 20$ with grid points $N = 100$, gave sufficient accuracy for the spectral relaxationmethod. The effects of the fluid parameters such as the thermophoresis parameter N_t, the Brownian motion N_b on thevelocity, temperature and nanoparticle profiles

have beendetermined.

Table 1 Effects of S, Q on $f''(0)$ when $Nt = 0:5$, $Nb = 0:5$, $Pr = 10$ and $Le = 10$.

		SRM	QLM	
S	Q		Ord 7	Ord 8
0.2	0.1	0.8310757	0.8310757	0.8310757
0.4	0.1	0.8640531	0.8640531	0.8640532
0.6	0.1	0.8959227	0.8959227	0.8959227
0.8	0.1	0.9263125	0.9263125	0.9263125
1.0	0.1	0.9551785	0.9551785	0.9551785
1.2	0.1	0.9825941	0.9825941	0.9825941
1.4	0.1	1.0086687	1.0086687	1.0086687
1.6	0.1	1.0335168	1.0335168	1.0335168
1.8	0.1	1.0572473	1.0572473	1.0572473
2.0	0.1	1.0799590	1.0799590	1.0799590
0.2	0.1	0.8310757	0.8310757	0.8310757
0.2	0.2	0.7746540	0.7746540	0.7746540
0.2	0.3	0.7393373	0.7393373	0.7393375
0.2	0.4	0.7135600	0.7135600	0.7135601
0.2	0.5	0.6932968	0.6932968	0.6932969
0.2	0.6	0.6766463	0.6766463	0.6766463
0.2	0.7	0.6625540	0.6625539	0.6625540
0.2	0.8	0.6503734	0.6503734	0.6503734
0.2	0.9	0.6396800	0.6396800	0.6396800
0.2	1.0	0.6301808	0.6301809	0.6301809

Table 2.Effects of S, Q, Nb and Nt on $-\theta'(0)$ when $Pr = 10$ and $Le = 10$.

		SRM	QLM	
S	Q		Ord 7	Ord 8
0.2	0.1	0.8310757	0.8310757	0.8310757
0.4	0.1	0.8640531	0.8640531	0.8640532
0.6	0.1	0.8959227	0.8959227	0.8959227
0.8	0.1	0.9263125	0.9263125	0.9263125
1.0	0.1	0.9551785	0.9551785	0.9551785
1.2	0.1	0.9825941	0.9825941	0.9825941
1.4	0.1	1.0086687	1.0086687	1.0086687
1.6	0.1	1.0335168	1.0335168	1.0335168
1.8	0.1	1.0572473	1.0572473	1.0572473
2.0	0.1	1.0799590	1.0799590	1.0799590
0.2	0.1	0.8310757	0.8310757	0.8310757
0.2	0.2	0.7746540	0.7746540	0.7746540
0.2	0.3	0.7393373	0.7393373	0.7393375
0.2	0.4	0.7135600	0.7135600	0.7135601
0.2	0.5	0.6932968	0.6932968	0.6932969
0.2	0.6	0.6766463	0.6766463	0.6766463
0.2	0.7	0.6625540	0.6625539	0.6625540
0.2	0.8	0.6503734	0.6503734	0.6503734
0.2	0.9	0.6396800	0.6396800	0.6396800
0.2	1.0	0.6301808	0.6301809	0.6301809

In order to have a sense of the accuracy and reliability of the spectral relaxation method, benchmark results were obtained. Tables (1) and (2) give a comparison between the results obtained using the spectral relaxation method and the quasi-linearization technique. The two sets of results are comparable up to six decimal places for all orders of the SRM from order five onwards.

Table (1) shows the effects of the unsteadiness and couple stress parameters on the skin-friction

coefficient. It is evident that increasing S leads to an increase in the skin frictioncoefficient. On the other hand, increasing Q leads to increases in skin friction coefficient. Table (2) shows the effects of S, Q, N_t and N_b on the Nusselt number. Here the Nusselt number increases as both the unsteadiness parameter and the couple stress parameter increase. We observe that increasing the thermophoresis parameter N_t increases the heat transfer coefficients increasewhile no effect occurs as the Brownian motion parameter increases.
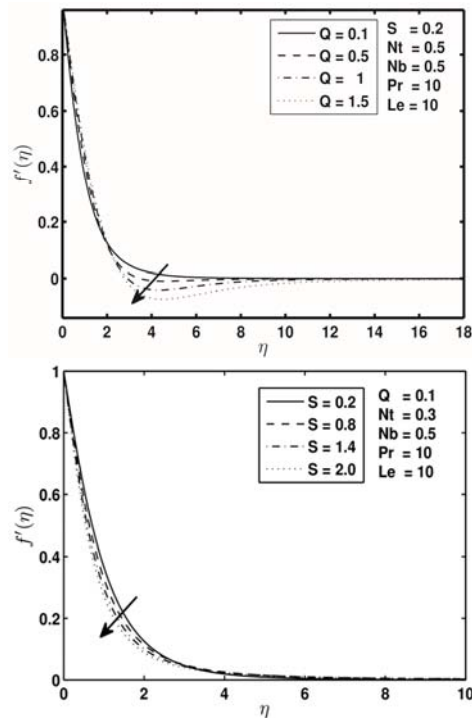
Fig. 2. Effect of the couple stress parameter Q and the unsteadiness parameter S on $f(\eta)$ for $Nt = 0.5$, $Nb = 0.5$, $Pr = 10$ and $Le = 10$.

Figure 2 shows the effect of the couple stress parameter$Q$ and the unsteadiness parameter S on velocity profilesrespectively within the boundary layer. We observe that, asexpected, strengthening the couple stress slows down the fluid motion due to an increasing drag force which is equivalent to an apparent decrease in the fluid viscosity. The velocity decreases with increasing Q until we obtain back flow in the range $2 \leq \eta \leq 8$. We also observe that the unsteadiness parameters lows the motion of the fluid within the boundary layer. It is clear that the boundary layer thickness reduces with increasing$S$.

Figure 3 shows the effect of the couple stress parameter Q on the temperature and mass volume fraction profiles respectively. Increasing Q leads to an increase in the thicknessof both the thermal and mass volume fraction boundary layers, henceincreasing Q reduces both the temperature and the mass volumefraction within the boundary layer.
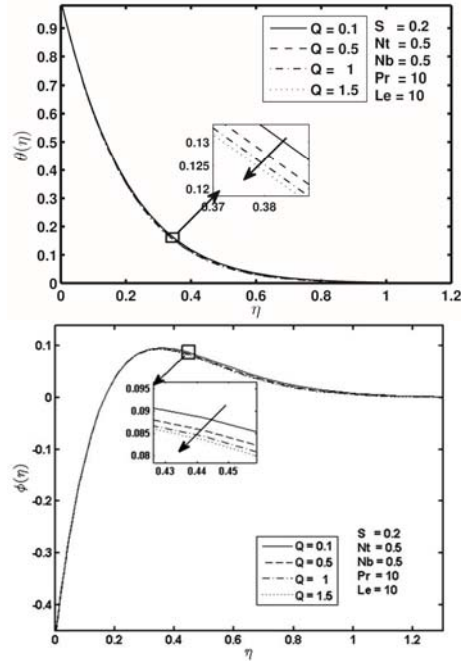

Fig. 3. Effect of the couple stress parameter Q on $\theta(\eta)$ and $\phi(\eta)$ for $S = 0.2$, $Nt = 0.5$, $Nb = 0.5$, $Pr = 10$ and $Le = 10$.
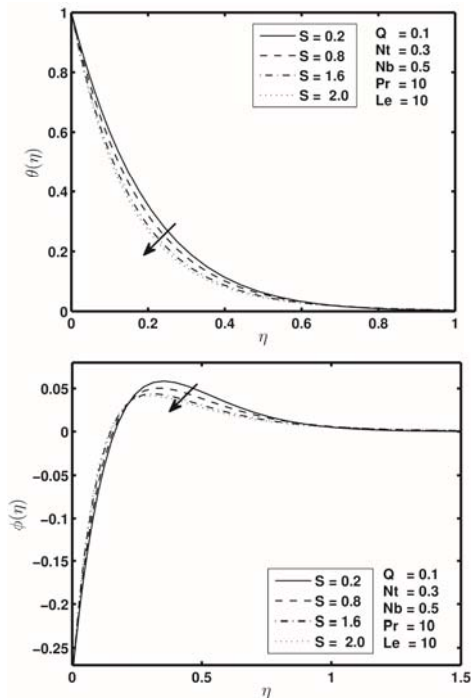

Fig. 4. Effect of the unsteadiness parameter S on $\theta(\eta)$ and $\phi(\eta)$ $Q = 0.1$, $Nt = 0.3$, $Nb = 0.5$, $Pr = 10$ and $Le = 10$.

The effect of the unsteadiness parameter S on the temperature andmass volume fraction are shown in Figure 4. We observe thatas S increases, the boundary layer velocity decreases causing adecrease in the heat and nanoparticle transfer

rates, hence the temperature and the nanoparticle inside boundary layer reduce. The influence of the thermophoresis parameter N_t on the temperature and nanoparticle profiles is given in Figure 5. Fast flowaway from the stretching surface exists due to the thermophoresis force generated by the temperature gradient. Therefore as N_t increases more a heated fluid travel away from the surface, hencethe temperature within the boundary layer increases. The fast flowfrom the stretching sheet carries with it nanoparticles leading to an increase in the mass volume fraction boundary layer thickness.
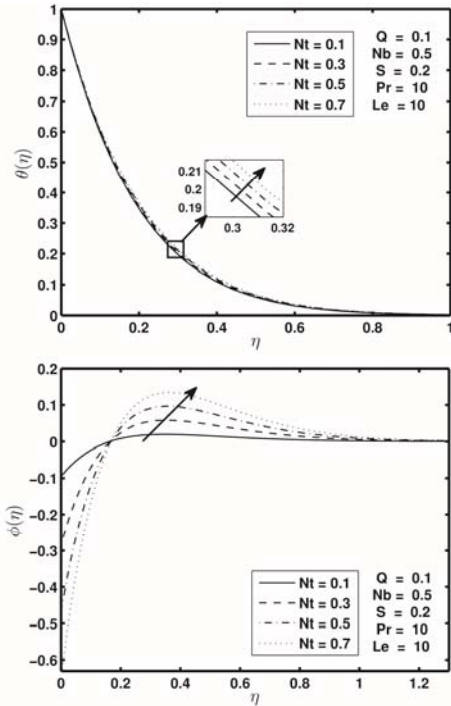

Fig. 5. Effect of the thermophoresis parameter Nt **on** $\theta(\eta)$ **and** $\phi(\eta)$ **for** $Q = 0, 1, \ S = 0, 2,$ $Nb = 0.5, Pr = 10$ **and** $Le = 10.$

5.   CONCLUSION

In this paper we have studied the flow of an unsteady nanofluid subject to couple stress effects. Numerical solutions of the equations governing the flow were found using the spectral relaxation method (SRM). The validation of the numerical results was done via a careful comparison between the solutions obtained using

The effect of the random motion of nanoparticles suspended in the fluid on the nanoparticle volume fraction is shown in Figure 6. It is evident that increasing N_b leads to a decrease in the mass volume fraction. Moreover, Figure 6illustrates the effect of the Lewis number Le on the mass volumefraction within boundary layer. Increasing Le leads to a decreasein the nanoparticle volume fraction within the thermal boundarylayer, this, in turn, leads to a decrease in the mass volume
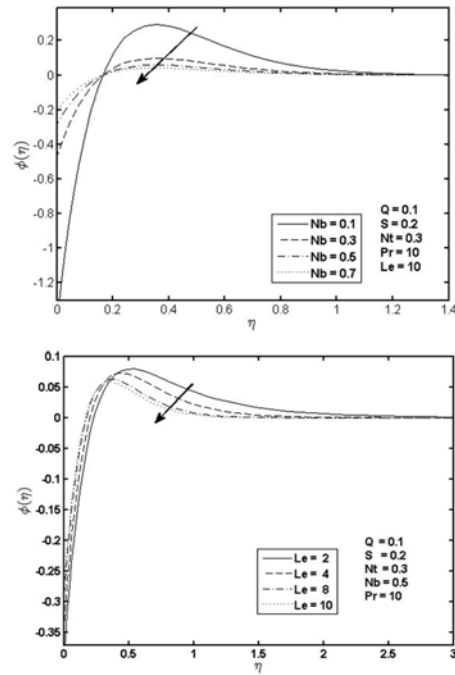
fraction gradient at the sheet surface.

Fig. 6. Effect of the Brownian motion parameter Nb **and the Lewis** $number \ Le$ **on** $\phi(\eta)$ **for** $Q =$ $0.1, \ S = 0.2, \ Nt = 0.5$ **and** $Pr = 10.$
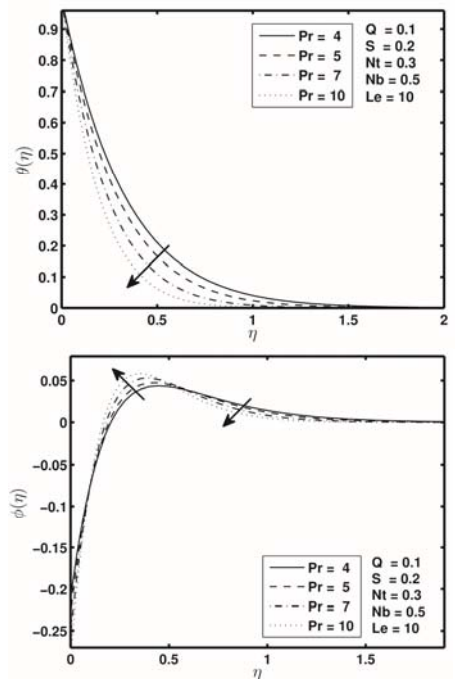
Fig. 7. Effect of the Prandtl number Pr **on** $\theta(\eta)$ **and** $\phi(\eta)$ **for** $Q = 0, 1, \ S = 0, 2, \ Nt = 0.5, \ Nb =$ 0.5 **and** $= 10.$

Figure 7 illustrates the variation of the temperature profile $\theta(\eta)$ and mass volume fraction profile $\phi(\eta)$ for some values of Prandtl number Pr. The results shows that increasing Pr reduces the

temperature profile, while the oppositeresults occurs when we vary the mass volume fraction with Pr.

The results in Figures 3 - 7 show that the nanoparticle volume fraction profiles starts from negative values and later become positive. This, as explained in Kuznetsov and Nield (2010b),is due to the fact the effect of thermophoresis is such that an elevation (above the ambient value of the surface temperature)results in a depression in the relative value of the nanoparticle fraction at the sheet.

the spectral relaxation and the quasi-linearization methods. We have presented the results graphically in order to illustrate the effects of various fluid parameters on the velocity, thermal and nanoparticle volume fraction profiles. The nanoparticle profiles are initially negative and become positive due to the effect of thermophoresis. The velocity is reduced by increasing the unsteadiness parameter. The temperature as well as the mass volume fraction decrease with an increase in the unsteadiness parameter. The stronger couple stress reduces the nanofluid velocity, as well as increasing the thickness of both the thermal and mass volume fraction boundary layers. The effect of the Brownian motion on the mass volume fraction within the boundary is much more significant rather than on the temperature.

REFERENCES

Ahmad, S. and I. Pop (2010). Mixed convection boundary layer flow from a vertical flat plate embedded in a porous medium filled with nanofluids. *International Communications in Heat and Mass Transfer* 37, 987-991.

Bachok, N., A. Ishak and I. Pop (2010). Boundary-layer flow of nanofluids over a moving surface in a flowing fluid. *International Scientific Journal Thermal Science* 49, 1663-1668.

Buongiorno, J. (2006). Convective transport in nanofluids. *ASME Jouraenal Heat Transfer* 128, 240-250.

Daungthongsuk, W. and S. Wongwises (2007). A critical review of convective heat transfer nanofluids. *Renewable and Sustainable Energy Reviews* 11, 797-817.

Daungthongsuk, W. and S. Wongwises (2007). nanofluidover a stretching sheet inthe presence stretching sheet inthe presence thermathermalradiation，*Journal of Molecular Liquids* 198，234–238.

Devakar, M. and T. Iyengar (2010). Run up flow of a couple stress fluid between parallel plates. *Nonlinear Analy-sis: Modelling and Control* 15, 29-37.

Devakar, M. and T. K. V. Iyengar (2010). Run up flow of a couple stress fluid between parallel plates. *Nonlinear Analysis: Modelling and Control* 15, 29-37.

Hayat, T., M. Mustafa, Z. Iqbal and A. Alsaedi (2013). Stagnation point flow of couple stress fluid with melting heat transfer. *Applied Mathematics and Mechanics* 34, 167-176.

Khan, N. A., A. Mahmood and A. Ara (2013). Approximate solution of couple stress fluid with expanding or contracting porous channel. *Engineering Computations* 30, 399-408.

Khan,W. A. and I. Pop (2010). Boundary layer flow of a nanofluid past a stretching sheet. *International Journal Heat Mass Transfer* 53, 2477-2483.

Kuznetsov, A. V. and D. A. Nield (2010a). Effect of local thermal non-equilibrium on the onset of convection in a porous medium layer saturated by a nanofluid. *Transportation in Porous Media* 83, 425-436.

Kuznetsov, A. V. and D. A. Nield (2010b). Natural convective boundary layer flow of a nanofluid past a vertical plate. *International Scientific Journal Thermal Science* 49, 243-247.

Kuznetsov, A. V. and D. A. Nield (2014). Natural convective boundary layer flow of a nanofluid past a vertical plate: A revised model. *International Journal of Thermal Sciences* 77, 126-129.

Malashetty, M. S., I. Pop, P. Kollur and W. Sidram (2012). Soret effect on double diffusive convection in a Darcy porous medium saturatedwith a couple stress fluid. *International Journal of Thermal Sciences* 53, 130-140.

Motsa, S. S., P. G. Dlamini and M. Khumalo (2012). Solving hyperchaotic systems using the spectral relaxation method. *Abstract and Applied Analysis,* V 203461,18.

Motsa, S. S., P. G. Dlamini and M. Khumalo (2013). On spectral relaxation method approach for steady von Kármán flow of a Reiner-Rivlin fluid with Joule heating, viscous dissipation and suction or injection. *Central European Journal of Physics 11*, 363-374.

Nadeem, S. and S. Akram (2011). Peristaltic flowof a couple stress fluid under the effect of induced magnetic field in an asymmetric channel. *Archive of Applied Mechanics* 81, 97-109.

Nield, D. A. and A. V. Kuznetsov (2009). The Cheng Minkowycz problem for natural convective boundary layer flow in a porous medium saturated by nanofluids. *International Journal Heat Mass Transfer* 52, 5792-5795.

Nield, D. A. and A. V. Kuznetsov (2014a). Thermal instability in a porous medium layer saturated by a nanofluid: A revised model. *International Journal of Heat and Mass Transfer* 68, 211-214.

Nield, D. A. and A. V. Kuznetsov (2014b). Forced convection in a parallel-plate channel occupied by a nanofluid or a porous medium saturated

by a nanofluid. *International Journal of Heat and Mass Transfer* 70, 430-433.

Nield, D. A. and A. V. Kuznetsov (2014c). The onset of convection in a horizontal nanofluid layer of finite depth: A revised model. *International Journal of Heat and Mass Transfer* 77, 915-918.

Oztop, H. F. and E. Abu-Nada (2008). Numerical study of natural convection in partially heated rectangular enclosures filled with nanofluids. *International Journal Heat Fluid Flow* 29, 1326-1336.

Oztop, H. F. and E. Abu-Nada (2008). Numerical study of natural convection in partially heated rectangular enclosures filled with nanofluids. *International Journal Heat Fluid Flow* 29, 1326-1336.

Ramana Murthy, J. V. and G. Nagaraju (2009). Flow of a couple stress fluid generated by a circular cylinder subjected to longitudinal and torsional oscillations. *Contemporary Engineering Sciences* 2, 451-461.

Ramzan, M., M. Farooq, A. Alsaedi and T. Hayat (2013). MHD threedimensional flow of couple stress fluid with Newtonian heating. *The European Physical Journal Plus* 128, 49.

Rashidi, M., N. Vishnu Ganesh, A. Abdul Hakeem and B. Ganga (2014). Buoyancy effect on MHD flow of

Sinha, P. and C. Singh (1984). Effects of couple stresses on the blood flow through an artery with mild stenosis. *Biorheology* 21, 303-315.

Stokes, V. K. (1966). Couple stresses in fluids. *Physics of Fluids* 9, 1709-1715.